Journal of Materials Science and Chemical Engineering, 2025, 13(6), 35-46
https://www.scirp.org/journal/msce
ISSN Online: 2327-6053
ISSN Print: 2327-6045

Preparation of a Fe_2O_3/C Catalyst and Its Performance in Catalytic Reduction of *o*-Bromonitrobenzene to *o*-Bromoaniline Using Hydazine Hydrate

Hui Fang, Ruishen Xie, Chundong Mi, Aiquan Jia, Qianfeng Zhang*

Institute of Molecular Engineering and Applied Chemistry, Anhui University of Technology, Ma'anshan, China
Email: *zhangqf@ahut.edu.cn

How to cite this paper: Fang, H., Xie, R.S., Mi, C.D., Jia, A.Q. and Zhang, Q.F. (2025) Preparation of a Fe_2O_3/C Catalyst and Its Performance in Catalytic Reduction of *o*-Bromonitrobenzene to *o*-Bromoaniline Using Hydazine Hydrate. *Journal of Materials Science and Chemical Engineering*, **13**, 35-46.
https://doi.org/10.4236/msce.2025.136003

Received: May 16, 2025
Accepted: June 24, 2025
Published: June 27, 2025

Abstract

The aim of this study was to develop an efficient Fe_2O_3/C catalyst for the catalytic reduction of *o*-bromonitrobenzene by hydrazine hydrate to give *o*-bromoaniline. Activated carbon was used as the carrier and its catalytic activity was enhanced by loading it with Fe_2O_3. Different preparation methods and reaction conditions were used to optimize the morphology and performance of the catalysts. It was found that the Fe_2O_3/C catalyst prepared by a one-step hydrothermal method after 10 h hydrothermal reaction conditions possessed the highest activity and cycling stability. Results of analytical investigations showed that the catalyst was well dispersed on the activated carbon, and the pore structure was conducive to enhancing the catalytic reduction. For *o*-bromonitrobenzene, high conversion was finally achieved, providing a reference for the applications of this type of catalyst in the field of catalytic reductions.

Keywords

Fe_2O_3/C catalyst, *o*-Bromonitrobenzene, Catalytic Reduction, Hydrothermal Method, Activated Carbon

1. Introduction

With the development of the chemical industry, many organic compounds containing halogen substituents and nitro groups have been widely used in areas such as pharmaceuticals, pesticides and dyes. However, these compounds are difficult to degrade naturally due to their highly chemical stability. Owing to their high toxicity, and their accumulation in the environment, these chemicals pose a seri-

ous threat to the ecosystem and human health. As a representative of such organic pollutants, *o*-bromonitrobenzene is a prominent example which accumulates in water and soil. Both the nitro(-NO_2) and bromo(-Br) substituents are difficult to be degraded and removed by microorganisms under natural conditions. In order to reduce its negative impact on the environment, the development of effective catalytic reduction methods to convert it into less harmful products such as *o*-bromoaniline has become a hot research topic.

Currently, the catalytic conversion of *o*-bromonitrobenzene into the corresponding aniline by reductants mainly relies on transition metal catalysts, such as palladium (Pd), platinum (Pt), nickel (Ni) and other noble metal catalysts [1] [2]. Although these catalysts exhibit good catalytic activity and selectivity, they are expensive, limited in their resources, and prone to deactivation during the reaction process, which limits their wide application. Therefore, the exploration of low-cost, highly efficient and stable non-precious metal catalysts has gradually become a research priority for solving such environmental problems.

Among the existing studies on non-precious metal catalysts, iron-based catalysts have gradually attracted the attention of scholars because of their good redox properties, wide resource distribution, and low cost [3]-[7]. For example, it has been shown that iron oxide (Fe_2O_3) has strong redox cycling properties and can effectively participate in the reduction reaction of organic pollutants [8]. However, when Fe_2O_3 is used alone as a catalyst, it usually suffers from poor dispersion, easy agglomeration, and suboptimal catalytic efficiency. These drawbacks make the application of Fe_2O_3 in catalytic reduction reactions somewhat limited. To overcome these problems, many researchers have tried to load Fe_2O_3 onto different carriers to improve its dispersion and catalytic activity.

Three mesoporous carbon-based materials, activated carbon (C), carbon black and graphene, are often used as carriers for the load of metal catalysts, which have a wide range of applications for environmental protection, catalytic reduction, etc. [9]. Among many possible carriers, activated carbon is widely used for catalyst preparation because of its large specific surface area, easy surface modification, porous structure and good stability [10]-[12]. Activated carbon is a highly porous carbon material synthesized by physical and chemical processes [13]. The highly porous nature of activated carbon gives it excellent thermal stability ensuring the durability and reliability of the catalyst [14]. Activated carbon not only provides a large number of active sites, but also enhances the performance of the catalyst by forming synergistic interactions with the loaded active components through its abundant surface functional groups. The results show that the catalytic activity of activated carbon on metal can be significantly improved in organic reduction reaction [15] [16]. However, most of the current studies have focused on the reduction of other nitro-containing compounds, and the studies on the reduction of *o*-bromonitrobenzene are still relatively few [17].

An iron oxide/activated carbon (Fe_2O_3/C) composite catalyst prepared using a hydrothermal method was employed in this study. The hydrothermal method, as a

mild preparation method, not only allows a uniform dispersion of Fe_2O_3 on activated carbon, but also promotes the formation of functional groups on the surface of the activated carbon, which enhances the interaction between Fe_2O_3 and the activated carbon. With this catalyst, high conversion rates were achieved under certain reaction conditions. Good catalytic activity was maintained after multiple recycling.

2. Experimental Section

2.1. Instruments and Reagents

The ASAP-2460 nitrogen adsorption-desorption analyzer was used to analyze the specific surface area, pore volume, and pore size distribution of the samples. Nitrogen adsorption-desorption isotherm data were obtained at 77 K. The specific surface area and pore size distribution were calculated using the Brunauer-Emmett-Teller (BET) equation and the Barret-Joyner-Halenda (BJH) model. Before testing, the samples were pre-treated by vacuum drying at 200˚C for 7 h.

The surface of the product was observed and analyzed by FEI Nova NanoSEM 430 field emission scanning electron microscope (SEM). The Raman spectroscopy (Raman) was used to study the chemical structure, phase and morphology of the catalyst by in Via laser confocal Raman spectrometer from the United Kingdom's Renishaw company.

Using the D8 Advance diffractometer from Germany's Bruker company, X-ray diffraction (XRD) patterns were recorded under conditions of 40 kV tube voltage and 30 mA tube current with Cu-K_α radiation. Fourier transform infrared spectroscopy (FT-IR) was performed using a Thermo Scientific Nicolet iS50 instrument to evaluate the chemical bonding analysis of the sample. Thermogravimetric analysis (TG) was conducted using a Netzsch STA 4449 F3 instrument in N_2 atmosphere to study the thermal stability of the catalyst and perform quantitative analysis. X-ray photoelectron spectroscopy (XPS) was used with a Thermo Scientific K-Alpha instrument to investigate the chemical composition and valence of elements in the sample.

The MSQ8100 model GC/MS gas chromatography-mass spectrometry instrument of Shanghai Shunyu Hengping Scientific Instrument Co., Ltd. was used to carry out quantitative and qualitative analysis of the products of catalytic experiments.

The reagents used were *o*-bromonitrobenzene, ferric nitrate hydrate ($Fe(NO_3)_3{\cdot}9H_2O$), activated charcoal, anhydrous ethanol, and hydrazine hydrate ($N_2H_4{\cdot}H_2O$), which were purchased from commercial sources with high purity.

2.2. Preparation of Catalyst Fe_2O_3/C

2.2.1. One-Step Hydrothermal Synthesis

Preparation of Fe_2O_3/C: 3.12 g of $Fe(NO_3)_3{\cdot}9H_2O$ was dissolved in 30 mL of deionized water and the solution stirred for 15 min, before 1.4 g of activated charcoal was added and stirring continued for 30 min. The mixture was transferred to a pressure reactor, where the hydrothermal reaction temperature was set at 180˚C for 8 h, 10 h

and 12 h. 180˚C was chosen as the reaction temperature for the following reasons. Firstly, the activated carbon can maintain the stability of the pore structure in a hydrothermal environment of less than 200˚C, avoiding the decrease of specific surface area caused by high temperature collapse. Secondly, the overgrowth of Fe_2O_3 particles can be suppressed at 180˚C, and homogeneous dispersed particles can be obtained (carrier domain limiting effect is enhanced). The hydrothermal time can directly affect the Fe_2O_3 particle size, which in turn determines the number of catalytic active sites. Hydrothermal time less than 8 h will lead to too small Fe_2O_3 particles, which are easy to sinter and deactivate. Hydrothermal time greater than 12 h will easily lead to agglomeration of Fe_2O_3 particles. Meanwhile, the pore structure of the activated carbon may collapse or the surface may oxidize under the prolonged hydrothermal environment. After the reaction is over, wait for the reactor to cool to room temperature, filter the reaction liquid to get the filter cake, and wash the filter cake with water and ethanol several times until the washing liquid is clear, and then put it into a 60˚C drying oven to dry for 3 h.

2.2.2. Two-Step Hydrothermal Synthesis

Preparation of Fe_2O_3: Add 5 g $Fe(NO_3)_3{\cdot}9H_2O$ to a beaker containing 25 mL deionized water. Stir at room temperature for 15 min, then transfer the reaction mixture to a reactor and subject it to a hydrothermal reaction at 180˚C for 10 h. Allow the reactor to cool to room temperature, filter the reaction mixture to obtain a filtrate, and wash the filtrate multiple times with water and ethanol until the wash solution is clear. Finally, dry the filtrate in an oven at 60˚C for 3 h.

Preparation of Fe_2O_3/C: Weigh 0.3 g of prepared Fe_2O_3 and add it to a beaker containing 20 mL of deionized water. Stir at room temperature for 15 min, then add 0.7 g of activated carbon while stirring, and continue stirring at 30˚C for 1 h. Filter the reaction mixture to obtain a filter cake, which is then washed multiple times with water and ethanol until the wash solution is clear. Finally, dry the filter cake in an oven at 60˚C for 3 h.

3. Catalyst Characterization

3.1. XRD Analysis

Powder X-ray diffraction was used to study the crystalline phase of Fe_2O_3. **Figure 1** shows the XRD patterns of the catalyst Fe_2O_3/C synthesized under different hydrothermal conditions, and the peaks located near 24.1˚, 33.0˚, 35.6˚, 40.8˚, 49.5˚, and 54.0˚ are the characteristic diffraction lines from Fe_2O_3. The intensity and width of the peaks changed with the increase of hydrothermal reaction time, but the position of the peaks did not change. The intensity of the peaks at 33.0˚ and 54.0˚ became lower and the width of the peaks became larger when the reaction time was from 8 h to 10 h owing to the increase of the dispersion of Fe_2O_3 on the activated carbon. The intensity of these peaks became higher and the width of the peaks became smaller when the reaction time was from 10 h to 12 h, which means that the dispersion of Fe_2O_3 on the activated carbon decreased at this time. The experiments

showed that the best dispersion was achieved at a hydrothermal time of 10 h.

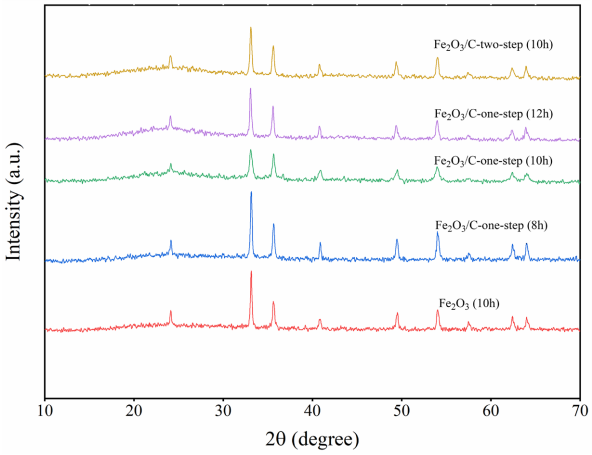

Figure 1. Powder XRD of Fe_2O_3/C prepared with different reaction times.

3.2. FT-IR and SEM Analysis

The FT-IR spectra of the catalysts are shown in **Figure 2**. They show only insignificant differences. Scanning electron microscopy was used to observe the surface morphology. The Fe_2O_3/C and the carrier activated carbon synthesized under different reaction conditions were characterized using SEM. The iron oxides were obviously loaded on the surface and in the pores of the activated carbon, resulting in the change of its surface morphology. **Figure 3(a)** shows the SEM image of the carrier activated carbon, in which there are fine particles on the surface and in the pores of the activated carbon, It is obvious from **Figure 3(b)**, that the iron oxide loading is not sufficient and some of the pores have less iron oxide loading. The iron oxide loading in the catalysts synthesized by the one-step method shown in **Figure 3(c)** and **Figure 3(d)** was sufficient, the carriers showed defects after the reaction time of 12 h, whereas the ones after 10 h did not, so the loading after the reaction time of 10 h was the best.

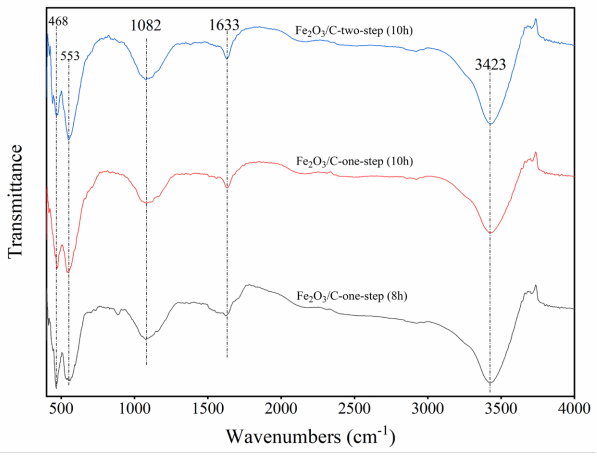

Figure 2. FT-IR spectra of Fe_2O_3/C obtained under different reaction conditions.

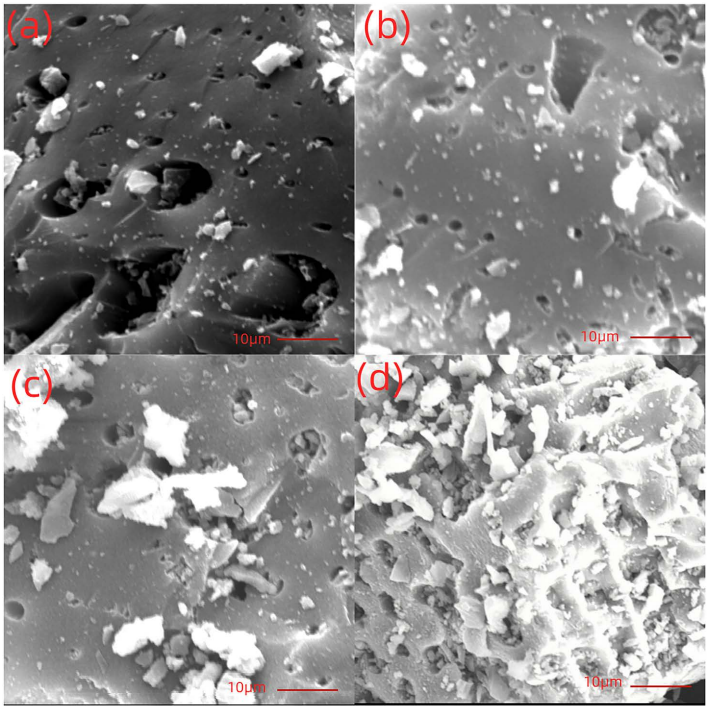

Figure 3. SEM of Fe_2O_3/C obtained under different reaction conditions, (a) Activated carbon; (b) Two-step synthesis; (c) One-step 10 h; (d) One-step 12 h.

3.3. BET Specific Surface Area and Pore Distribution Analysis

Nitrogen adsorption-desorption analysis was used to test the specific surface area and pore size. The BET adsorption isotherms in **Figure 4** (the specific parameters are listed in **Table 1**) show that the specific surface area of Fe_2O_3/C prepared by one-step method is significantly higher than that of two-step method. Observation reveals that all samples exhibit type IV isotherms as defined by IUPAC, which indicates the presence of irregular mesoporous (2~50 nm) structures in these samples. The specific surface area of the catalysts with a hydrothermal time of 10 h reaches 572 m^2/g, which provides larger active areas for the reaction.

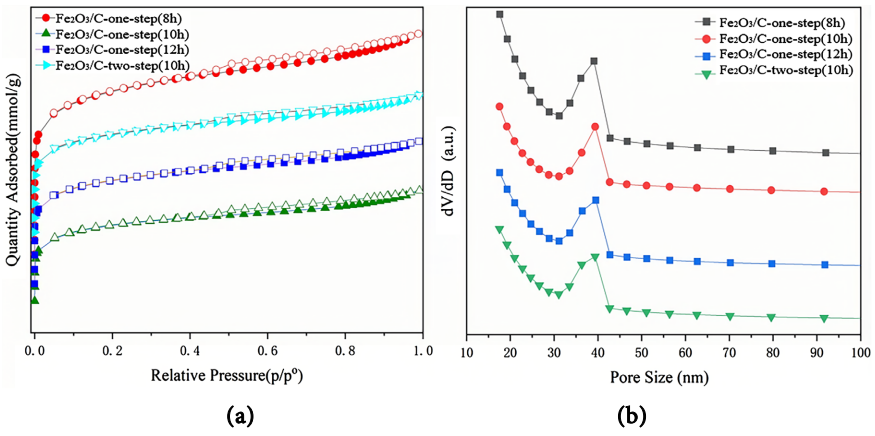

Figure 4. (a) N_2 adsorption-desorption curves of Fe_2O_3/C; (b) Pore distribution curves of Fe_2O_3/C.

Table 1. Specific surface area, pore volume, and average pore size of Fe_2O_3/C.

Sample	S_{BET} (m^2/g)	Pore volume (cm^3/g)	Average pore size (nm)
Fe_2O_3/C-two-step (10 h)	347.42	0.314	39.10
Fe_2O_3/C-one-step (8 h)	442.80	0.283	39.50
Fe_2O_3/C-one-step (10 h)	572.27	0.360	39.79
Fe_2O_3/C-one-step (12 h)	547.49	0.346	39.24

3.4. XPS Analysis

The XPS spectra of Fe_2O_3/C (**Figure 5**) showed that the valence state of Fe was mainly +3. The broad peaks of the Fe 2*p* orbitals proved the stable distribution of Fe_2O_3 on the surface of the catalyst, which indicated that the structure of the catalyst was stable and conducive to the enhancement of catalytic performance. As shown in **Figure 5**, the full spectrum of Fe_2O_3/C-one-step (10 h) and the XPS spectra of Fe 2*p* orbitals, **Figure 5(a)** shows that Fe_2O_3/C consists of Fe, O, and C elements. Using C 1*s* at 284.8 eV as a reference peak, the XPS spectrum of the Fe 2*p* orbital of the catalyst is shown in **Figure 5(b)**. Two broad peaks attributed to $Fe_{2p3/2}$ and $Fe_{2p1/2}$ were found at binding energies of 710.4 eV and 724.1 eV, respectively, and the values coincide with the eigenvalues, suggesting that the catalyst is shown to exist predominantly in the +3 valence form. In addition, satellite peaks of Fe_2O_3/C at binding energies 718.5 eV and 732.2 eV can be clearly seen.

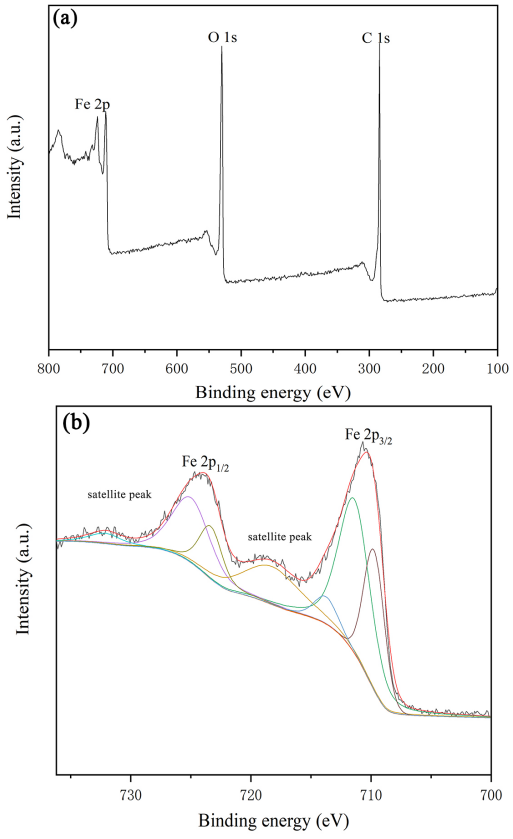

Figure 5. (a) XPS of Fe_2O_3/C-one-step (10 h); (b) XPS of Fe 2*p*.

3.5. TG Analysis

The thermal stability of the catalysts can be analyzed by TG mapping (in a nitrogen atmosphere). From **Figure 6**, it can be seen that the prepared catalysts all showed excellent thermal stability, with a small mass loss only below 100˚C, which may be related to the adsorbed water on the surface of the samples. There was no significant mass loss between 100˚C and 500˚C.

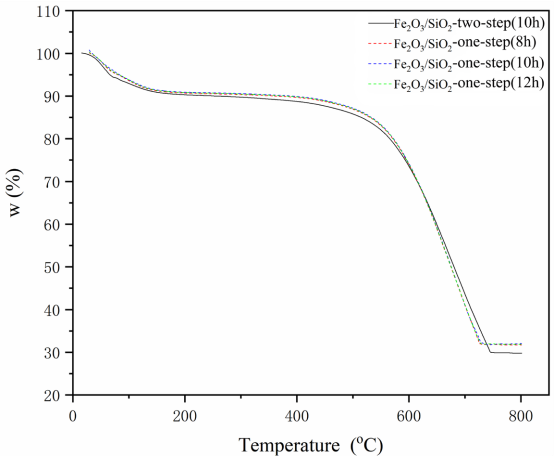

Figure 6. TG of Fe_2O_3/C.

4. Experimental Part

4.1. Evaluation of Catalytic Performance

Using $N_2H_4 \cdot H_2O$ as the hydrogen source and *o*-bromonitrobenzene as the reactant, catalytic hydrogenation reduction is carried out in an ethanol solution. The selection of hydrazine hydrate as a reducing agent over other common hydrogen donors (e.g., H_2, $NaBH_4$, formic acid, etc.) is based on its unique advantages in selective reduction of nitro groups, retention of halogen functional groups and mildness of reaction conditions. (1) Highly selective retention of halogen groups. The C-Br bond in *o*-bromonitrobenzene is easily broken by strong reducing agents (e.g., H_2/precious metals), resulting in dehalogenation by-products. In contrast, hydrazine hydrate reduces nitro by an electron transfer mechanism rather than a radical pathway, retaining the C-Br bond; (2) Convenience of low temperature operation at atmospheric pressure. H_2 reduction requires high-pressure equipment, and high temperatures may trigger dehalogenation or over reduction. The liquid phase reaction of hydrazine hydrate can be carried out at atmospheric pressure and low temperature, which significantly reduces energy consumption and safety risks; (3) Environmental friendliness. The by-products are only N_2 and H_2O, which is in line with the principle of green chemistry, and the atom utilization rate is up to 90%; (4) Synergistic effect with iron-based catalysts. The Fe^{3+}/Fe^{2+} redox cycle activates hydrazine to release reactive hydrogen and inhibits the excessive decomposition of hydrazine to produce reactive nitrogen species, which in turn leads to catalyst deactivation. Despite the toxicity challenges of hydrazine

hydrates, they are ideal for laboratory optimization.

The specific experimental steps are: add 10 mL of anhydrous ethanol to a 25 mL three-necked flask, then add 1.5 mL $N_2H_4 \cdot H_2O$, and under stirring, add 0.5 g of *o*-bromonitrobenzene, followed by 0.06 g of catalyst Fe_2O_3/C. The reaction is then refluxed at 80˚C for 3~5 h. The reaction mixture is filtered, and analyzed quantitatively and qualitatively using a gas chromatography-mass spectrometry (GS/MS) instrument to determine the catalytic conversion rate and selectivity.

The activity test results of the catalysts under different conditions are shown in Table 2. At a one-step hydrothermal reaction time of 10 h, the highest conversion rate of Fe_2O_3/C catalyzed product to *o*-bromoaniline was 83%, and the selectivity was over 98%.

Table 2. Results of Fe_2O_3/C catalyzed reduction of *o*-bromonitrobenzene by hydrazine hydrate with catalysts prepared under different reaction conditions[a].

Sample	Time (h)	Conversion (%)	Selectivity (%)
Fe_2O_3/C-one-step (8 h)	3	70	>98
Fe_2O_3/C-one-step (10 h)	3	83	>98
Fe_2O_3/C-one-step (12 h)	3	73	>98
Fe_2O_3/C-two-step (10 h)	3	70	>98

[a]Reaction conditions: 0.5 g *o*-bromonitrobenzene, 10 mL anhydrous ethanol, 1.5 mL hydrazine hydrate, 0.06 g catalyst, reaction temperature 80˚C.

4.2. Cycling Performance of the Catalysts

The cycling performance of the catalyst was evaluated by repeating the experiment six times. After the reaction, the catalyst was alternately washed with ethanol and water, and then dried in an oven at 100˚C. In order to better investigate the cycling performance of the catalyst, the amount of raw materials such as reaction substrate, hydrogen donor and ethanol and the reaction time were kept unchanged. As shown in Figure 7, the Fe_2O_3/C catalyst prepared by 10 h hydrothermal reaction method can maintain a conversion rate of more than 80% and good selectivity in six cycles.

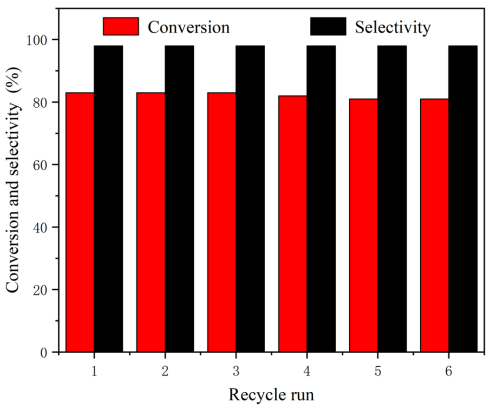

Figure 7. Results of cyclic experiments on the reduction of *o*-bromonitrobenzene by hydrazine hydrate catalyzed by Fe_2O_3/C.

5. Industrial Testing Necessity

Based on this, the Fe_2O_3/C catalyst has demonstrated activity potential at the laboratory stage, but has not yet been tested under strictly industrial conditions. In the future, a three-step process of continuous flow testing, lifetime analysis, and safety assessment will be required to move towards industrial applications. Validation may involve the following industrial scenarios: (1) Continuous flow experiments. Test the performance of the catalyst in the flow system by building a fixed-bed reactor (residence time, mass transfer effect, air velocity and pressure, etc. on the conversion rate); (2) Influence of feedstock impurities (industrial grade *o*-bromonitrobenzene containing sulfur/water and other impurities poisoning the catalyst); (3) Catalyst life and regeneration tests (>100 h stability, comparison of the effects of roasting (air) and pickling (HNO_3) on active regeneration performance); (4) Safety and economic analysis. Exploration of alternative reductants and assessment of the feasibility of H_2 or sodium format reduction routes.

6. Conclusions

In this study, Fe_2O_3/C catalysts with high catalytic activity were prepared and their catalytic performance for the reduction reaction of *o*-bromonitrobenzene with hydrazine hydrate was systematically investigated. The following conclusions can be drawn:

1) Different preparation methods have significant effects on the dispersion and stability of Fe_2O_3 on activated carbon. The XRD and SEM characterization showed that the Fe_2O_3/C catalyst prepared by a one-step method has higher dispersion and larger specific surface area, which is conducive to the formation of more active sites on the surface of the catalyst, thus enhancing the reaction rate and selectivity.

2) The catalytic activity of Fe_2O_3/C catalyst prepared by hydrothermal method was affected by different reaction times. When the reaction time is 10 h, the dispersion of Fe_2O_3 on the surface of activated carbon is most uniform. If the time is too long or too short, the dispersion is reduced, thus affecting the catalytic activity.

3) Activated carbon as a carrier not only provides a large surface area and pore structure, but also synergizes with Fe_2O_3 to enhance its catalytic performance. The results of the characterization by FT-IR and XPS indicated that the surface groups of activated carbon. This distribution not only helps to form more active sites, but also prevents the agglomeration of Fe_2O_3, improving the activity and stability of the catalyst.

The Fe_2O_3/C catalyst effectively accelerates the reduction of *o*-bromonitrobenzene with hydrazine hydrate to produce the target product *o*-bromoaniline. The Fe_2O_3/C catalyst presented in this study provides an effective solution for the catalytic reduction of *o*-bromonitrobenzene by hydrazine hydrate. Future studies, it will be tried to apply this catalyst for the reduction of other nitrogen-containing organic compounds to further expand its application scope.

Acknowledgements

This project was supported by the National Natural Science Foundation of China (21372007).

Conflicts of Interest

The authors declare no conflicts of interest regarding the publication of this paper.

References

[1] Govindan, K., Noel, M. and Mohan, R. (2015) Removal of Nitrate Ion from Water by Electrochemical Approaches. *Journal of Water Process Engineering*, **6**, 58-63. https://doi.org/10.1016/j.jwpe.2015.02.008

[2] Wang, Q., Zhao, X., Zhang, J. and Zhang, X. (2015) Investigation of Nitrate Reduction on Polycrystalline Pt Nanoparticles with Controlled Crystal Plane. *Journal of Electroanalytical Chemistry*, **755**, 210-214. https://doi.org/10.1016/j.jelechem.2015.08.005

[3] Liu, T., Zhang, B. and Sun, L. (2018) Iron-Based Molecular Water Oxidation Catalysts: Abundant, Cheap, and Promising. *Chemistry—An Asian Journal*, **14**, 31-43. https://doi.org/10.1002/asia.201801253

[4] Pang, Y., Kong, L., Chen, D. and Yuvaraja, G. (2019) Rapid Cr(VI) Reduction in Aqueous Solution Using a Novel Microwave-Based Treatment with MoS_2-$MnFe_2O_4$ Composite. *Applied Surface Science*, **471**, 408-416. https://doi.org/10.1016/j.apsusc.2018.11.180

[5] Guan, X., Du, X., Liu, M., Qin, H., Qiao, J. and Sun, Y. (2020) Enhanced Trichloroethylene Dechlorination by Carbon-Modified Zero-Valent Iron: Revisiting the Role of Carbon Additives. *Journal of Hazardous Materials*, **394**, Article 122564. https://doi.org/10.1016/j.jhazmat.2020.122564

[6] Diao, Z., Qian, W., Lei, Z., Kong, L., Du, J., Liu, H., *et al.* (2019) Insights on the Nitrate Reduction and Norfloxacin Oxidation over a Novel Nanoscale Zero Valent Iron Particle: Reactivity, Products, and Mechanism. *Science of The Total Environment*, **660**, 541-549. https://doi.org/10.1016/j.scitotenv.2019.01.037

[7] Liu, J., Diao, Z., Liu, C., Jiang, D., Kong, L. and Xu, X. (2018) Synergistic Reduction of Copper (II) and Oxidation of Norfloxacin over a Novel Sewage Sludge-Derived Char-Based Catalyst: Performance, Fate and Mechanism. *Journal of Cleaner Production*, **182**, 794-804. https://doi.org/10.1016/j.jclepro.2018.02.045

[8] Wang, H., Fan, W., Li, J., Tang, X., Qing, D. and Lu, J. (2025) Size Effect of Iron Oxide Nanocatalysts on Heavy Oil Viscosity Reduction through Catalytic Aquathermolysis. *Journal of Analytical and Applied Pyrolysis*, **186**, Article 106949. https://doi.org/10.1016/j.jaap.2025.106949

[9] Auer, E., Freund, A., Pietsch, J. and Tacke, T. (1998) Carbons as Supports for Industrial Precious Metal Catalysts. *Applied Catalysis A*: *General*, **173**, 259-271. https://doi.org/10.1016/s0926-860x(98)00184-7

[10] Boukoussa, B., Cherdouane, K.R., Zegai, R., Mokhtar, A., Hachemaoui, M., Issam, I., *et al.* (2024) Preparation of Activated Carbon-Metal Nanoparticle Composite Materials for the Catalytic Reduction of Organic Pollutants. *Surfaces and Interfaces*, **44**, Article 103622. https://doi.org/10.1016/j.surfin.2023.103622

[11] Pasel, J., Käßner, P., Montanari, B., Gazzano, M., Vaccari, A., Makowski, W., *et al.* (1998) Transition Metal Oxides Supported on Active Carbons as Low Temperature

Catalysts for the Selective Catalytic Reduction (SCR) of NO with NH_3. *Applied Catalysis B*: *Environmental*, **18**, 199-213. https://doi.org/10.1016/s0926-3373(98)00033-2

[12] Sanchis, I., Rodriguez, J.J., Mohedano, A.F. and Diaz, E. (2023) N-Doped Activated Carbon as Support of Pd-Sn Bimetallic Catalysts for Nitrate Catalytic Reduction. *Catalysis Today*, **423**, Article 114011. https://doi.org/10.1016/j.cattod.2023.01.018

[13] Rodríguez-Reinoso, F. and Molina-Sabio, M. (1998) Textural and Chemical Characterization of Microporous Carbons. *Advances in Colloid and Interface Science*, **76**, 271-294. https://doi.org/10.1016/s0001-8686(98)00049-9

[14] Jain, A., Balasubramanian, R. and Srinivasan, M.P. (2016) Hydrothermal Conversion of Biomass Waste to Activated Carbon with High Porosity: A Review. *Chemical Engineering Journal*, **283**, 789-805. https://doi.org/10.1016/j.cej.2015.08.014

[15] Li, H., Chen, X., Fu, P., Tang, B., Zhuansun, X., Sun, Z., *et al.* (2025) Synthesis of Metal and Nitrogen Co-Doped Activated Carbon Catalysts for the Co-Production of Monocyclic Aromatics and Hydrogen-Rich Gas from the Pyrolysis of Biomass and Plastic. *Energy*, **316**, Article 134652. https://doi.org/10.1016/j.energy.2025.134652

[16] Madhanagopal, G., Premalatha, K., Poovizhi, P.N., Sumithra, V., Mahalingam, S., Guganathan, L., *et al.* (2025) Effect of a Bimetal Mn/Zn Catalyst Supported on Activated Carbon for Selective Oxidation of Ethyl Lactate to Ethyl Pyruvate. *Carbon Trends*, **19**, Article 100472. https://doi.org/10.1016/j.cartre.2025.100472

[17] Wang, X., Liang, M., Liu, H. and Wang, Y. (2007) Selective Hydrogenation of Bromonitrobenzenes over Pt/γ-Fe_2O_3. *Journal of Molecular Catalysis A*: *Chemical*, **273**, 160-168. https://doi.org/10.1016/j.molcata.2007.04.004